Response Functions of Spiral Wave Solutions of the Complex Ginzburg-Landau Equation

I.V.Biktasheva[1], V.N.Biktashev[2]
Institute for Mathematical Problems in Biology,
142292 Pushchino, Moscow region, Russia

October 26, 1999

[1] Current address: School of Biomedical Sciences, University of Leeds, Leeds LS2 9JT, UK
[2] Current address: Applied Mathematics, M & O Building, University of Liverpool, Liverpool L69 7ZL, UK

Abstract

Dynamics of spiral waves in perturbed two-dimensional autowave media can be described asymptotically in terms of Aristotelean dynamics. We apply this general theory to the spiral waves in the Complex Ginzburg-Landau equation (CGLE). The RFs are found numerically. In this work, we study the dependence of RFs on parameters of the CGLE.

1 Introduction

Spiral waves are a specific form of self-organisation first discovered in the Belousov-Zhabotinsky reaction medium [1] and observed in various physical, chemical and biological systems; of the most practical importance is the cardiac muscle, where spiral waves underlie dangerous arrhythmias including fibrillation [2]. Usually they are studied using "reaction+diffusion" systems of partial differential equations,

$$\partial_t u = f(u) + D\nabla^2 u + \varepsilon h(u,x,t), \quad u, f \in \mathbb{R}^\ell,\ D \in \mathbb{R}^{\ell\times\ell},\ \ell \geq 2. \tag{1}$$

In unperturbed media, at $\varepsilon = 0$, we assume that a solution in the form of a steadily rotating wave exists:

$$u = U(\mathbf{r},t) = U\left(\rho(\mathbf{r}), \vartheta(\mathbf{r}) + \omega t\right). \tag{2}$$

This rotating wave will be a spiral wave, if $U(\rho,\phi) \approx \tilde{U}(\rho/\Lambda - \phi/2\pi)$ as $\rho \to \infty$, for a $\tilde{U}(\xi)$: mod (1), $\tilde{U} \not\equiv$ const. Then equiphase lines at large ρ are close to Archimedean spirals with pitch Λ.

If a spiral wave solution (2) exists, then

$$\tilde{u} = U\left(\rho(\mathbf{r}-\mathbf{R}), \vartheta(\mathbf{r}-\mathbf{R}) + \Theta\right), \tag{3}$$

where $\Theta = \omega t - \Phi$, is another solution for any constant $\mathbf{R}$, Φ. This is a spiral wave shifted in space by $\mathbf{R}$ and rotated by Φ, or, equivalently, shifted in time by Φ/ω. Thus, the unperturbed reaction-diffusion system has a three-dimensional manifold of spiral wave solutions, parametrised by two-dimensional vector $\mathbf{R}$ and phase Θ. The physical observability implies that this manifold is reasonably stable as a whole.

A perturbation $\varepsilon h \neq 0$ could be a slight inhomogeneity of the medium or explicit time-dependent external forcing. The typical effects of the perturbation on the stable invariant manifold of spiral waves are (i) displacement of the manifold, (ii) perturbed dynamics along this manifold. The latter is a slow change of previously constant parameters $\mathbf{R}$ and Φ, *i.e.* spatial and temporal drift of the spiral wave (the temporal drift is the shift of the rotation frequency),

$$\partial_t \Theta = \omega + \varepsilon F_0(\mathbf{R}, \Theta), \qquad \partial_t \mathbf{R} = \varepsilon \mathbf{F}_1(\mathbf{R}, \Theta). \tag{4}$$

The velocities F_0, $\mathbf{F_1}$ of these drifts, in the first approximation, are linear functionals of the perturbation. Both F_0 and $F_1 \equiv \mathbf{F}_{1,x} + i\mathbf{F}_{1,y}$, after sliding averaging over the spiral wave rotation period, can be expressed as

$$\bar{F}_n(t) = e^{in\Phi} \oint\limits_{t-\pi/\omega}^{t+\pi/\omega} \frac{\omega \mathrm{d}\tau}{2\pi} \iint\limits_{\mathbb{R}^2} \mathrm{d}^2\mathbf{r}\, e^{-in\omega\tau} \left\langle W_n \left(\rho(\mathbf{r}-\mathbf{R}), \vartheta(\mathbf{r}-\mathbf{R}) + \omega\tau - \Phi\right), h \right\rangle, \tag{5}$$

where

$$h = h\left(U\left(\rho(\mathbf{r}-\mathbf{R}), \vartheta(\mathbf{r}-\mathbf{R}) + \omega\tau - \Phi\right), \mathbf{r}, \tau\right), \qquad \mathbf{R} = \mathbf{R}(t), \quad \Phi = \Phi(t), \tag{6}$$

and W_n, $n = 0, \pm 1$ are the critical eigenfunctions,

$$L^+ W_n = -i\omega n W_n, \quad n = 0, \pm 1, \tag{7}$$

of the adjoint linearised operator

$$L^+ = D\nabla^2 + \omega\partial_\vartheta + \left(\frac{\partial f}{\partial u}\right)^T \Bigg|_{u=U(\mathbf{r})}, \tag{8}$$

chosen to be biorthogonal to the Goldstone modes,

$$\begin{aligned} V_0 &= -\partial_\vartheta U(\rho(\mathbf{r}), \vartheta(\mathbf{r}))|_{t=0}, \\ V_{\pm 1} &= -\frac{1}{2} e^{\mp i\vartheta} \left(\partial_\rho \mp i\rho^{-1}\partial_\vartheta\right) U(\rho(\mathbf{r}), \vartheta(\mathbf{r}))|_{t=0}. \end{aligned} \tag{9}$$

which are the critical eigenfunctions of the linearised operator,

$$L = D\nabla^2 - \omega\partial_\vartheta + \left(\frac{\partial f}{\partial u}\right) \Bigg|_{u=U(\mathbf{r})}. \tag{10}$$

We call $W_{0,1}$ the response functions (RFs). These functions, in the context of autowave vortices, were first introduced to describe the dynamics of twisted and bent three-dimensional scroll waves [3, 4], and then used to describe the

dynamics of the two-dimensional spiral waves in perturbed media [5]. Like the spiral wave solution themselves, the RFs can be found numerically. If neither the perturbation nor the RFs are localised in space, then the convolution integrals (5) may diverge. It was hypothesised in [4, 5] that typically in spiral waves, the RFs are essentially localised, *i.e.* quickly decay with the distance from the spiral rotation centre. The RFs were found and this hypothesis has been confirmed for a particular autowave model, the Complex Ginzburg-Landau equation (CGLE), at a particular choice of parameters, in [6]. Based on that result, the predictive ability of the theory has been tested in [7].

In this paper, we study the behaviour of the RFs in a broad region of the parametric space of CGLE. The considered region of the parameters was limited by the existence and stability of the spiral wave solutions. The conclusion is that in all the explored region, the localisation of the RFs persists.

2 Results

Perturbed Complex Ginzburg Landau Equation (CGLE) is a two-component reaction-diffusion system which is conveniently presented in the complex form:

$$\partial_t u = u - (1 - \mathcal{I}\alpha)u\,|u|^2 + (1 + \mathcal{I}\beta)\nabla^2 u + \varepsilon h \tag{11}$$

where $u \in \mathbb{C}$, $\alpha, \beta \in \mathbb{R}$. The imaginary unit $\mathcal{I}$ in this equation must be treated as a different mathematical entity from i of the general theory; *i.e.* we are working with an algebra of "bicomplex numbers", see [6] for details.

The steadily rotating spiral wave solutions to this equation have been studied by Hagan [8], and have the form

$$U(\mathbf{r}, t) = e^{\mathcal{I}(\vartheta + \omega t)} P(\rho) \tag{12}$$

where $P(\rho) = a(\rho)e^{\mathcal{I}\psi(\rho)} \in \mathbb{C}$ and ω solve a nonlinear eigenvalue problem

$$\begin{aligned} &(1 + \mathcal{I}\beta)\left(P'' + \frac{1}{\rho}P' - \frac{1}{\rho^2}P\right) + \left(1 - \mathcal{I}\omega - (1 - \mathcal{I}\alpha)|P|^2\right)P = 0, \\ &P(\rho \to 0) \propto \rho, \quad P(\rho \to \infty) \approx \sqrt{1 - k^2}\exp(\mathcal{I}k\rho + o(\rho))(1 + o(1)), \end{aligned} \tag{13}$$

where $k = k(\alpha, \beta)$ is the asymptotical wavenumber, changing sign at $\alpha + \beta = 0$, and $\omega = \alpha - \alpha k^2 - \beta k^2$. The response functions have the form [6]:

$$W_n = e^{(\mathcal{I} - in)\vartheta} Q_n(\rho) \tag{14}$$

where Q_n, $n = 0, 1$ are solutions to linear problems

$$\begin{aligned} &(1 - \mathcal{I}\beta)\left\{Q_n'' + \frac{1}{\rho}Q_n' + \frac{(\mathcal{I} - in)^2}{\rho^2}Q_n\right\} \\ &\qquad + \left\{1 + \mathcal{I}\omega - a^2\left[2(1 + \mathcal{I}\alpha) + (1 - \mathcal{I}\alpha)e^{2\mathcal{I}\psi}\mathcal{C}\right]\right\}Q_n = 0, \\ &|Q_n(\rho \to 0)| < \infty, \quad Q_n(\rho \to \infty) \to 0. \end{aligned} \tag{15}$$

Here $\mathcal{C}$ is the operator of $\mathcal{I}$-conjugation; W_1 and Q_1 are bicomplex-valued functions, each having four components.

We have studied numerically the behaviour of the solutions to the problem (13),(15) on the parameters α and β. We used the numerical procedure

described in [6], typically on the interval $\rho \in [0:50]$ with discretisation step $\Delta\rho = 0.07$. The parametric portrait of the CGLE is central symmetric in the (α, β) plane, so we consider only $\alpha \geq 0$ without loss of generality. The existence of localised RFs was considered established if the absolute values of the artificial eigenvalues (see [6]) were less than 10^{-3}.

The explored regions is shown in Fig. 1. The points at this figure mark the values of α and β at which the computations have been done and existence of localised RFs ensured. Solutions, corresponding to the selected points, are presented on subsequent figures. Point $(0.5, 0)$ was illustrated in [6, 7].

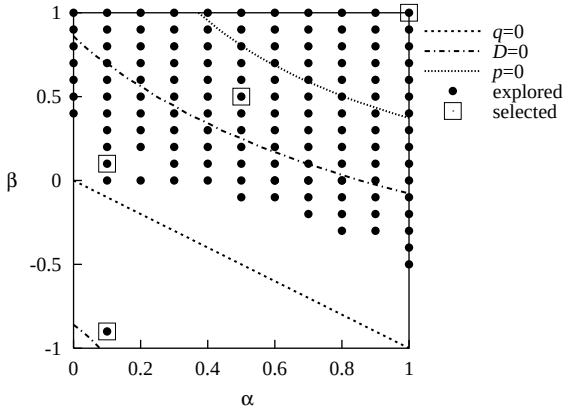

Figure 1: The explored region of (α, β) plane.

The expected decrease of Q_n at $\rho \to \infty$ implies that

$$Q_n(\rho) \propto e^{\lambda\rho}, \tag{16}$$

where λ is a root of the characteristic equation

$$\lambda^3 + p\lambda + q = 0 \tag{17}$$

with $\mathrm{Re}(\lambda) < 0$, typically the one with the least $|\mathrm{Re}(\lambda)|$. Here

$$p = 2\frac{\alpha\beta - 1 + k^2\left(3 + 2\beta^2 - \alpha\beta\right)}{1 + \beta^2}, \quad q = -4k\frac{(\alpha + \beta)(1 - k^2)}{1 + \beta^2}.$$

The problem for the RFs is properly posed, in the sense used in [6], if (17) has one positive root and two roots with negative real parts. This is fulfilled as long as $|k(\alpha, \beta)| < 1$, except on the line $\alpha + \beta = 0$, when one of the roots vanishes. The sign of k changes when crossing the line $\alpha + \beta = 0$. This is why the winding of the spiral at Fig. 2 is opposite to that on the other four figures. Near $\alpha + \beta = 0$, the asymptotic wavelength grows to infinity, and at intermediate ρ, the spiral is logarithmic rather than Archimedean [8]. This is indeed seen on Fig. 3. It can be seen that the critical root λ of the characteristic equation (17) becomes very small in this limit, $\lambda \propto -(\alpha + \beta)k$, where k, in turn, is exponentially small in $(\alpha + \beta)$ [8]. This makes the computations of the spiral waves and the RFs in the vicinity of this line more difficult. At this line, the CGLE becomes a quasi-gradient system, hence $L^+ \approx \bar{L}$, and so near it we may expect the RFs

W_n to become similar to the Goldstone modes V_n. In this limit, in the region $1 \ll \rho \ll k^{-1}$ the amplitude of V_0 remains approximately constant as well as that of U, while V_1 decays as ρ^{-1}. This is consistent with the behaviour of W_n seen on Fig. 3.

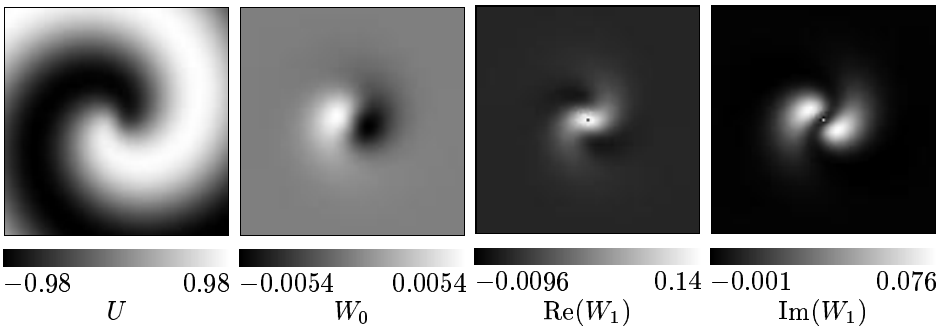

Figure 2: The spiral wave (U), temporal RF (W_0) and the i-real and i-imaginary components of the spatial RF (W_1), as density plots. Shown are the $\mathcal{I}$-real components of all four functions; the $\mathcal{I}$-imaginary components are the same functions rotated by $\pi/2$. Spatial region displayed on this and subsequent figures is $(x, y) \in [-20, 20] \times [-20, 20]$, with resolution 91×91 pixels. The homogeneous shades of grey on the peripheries of $W_{0,1}$ correspond to zero, *i.e.* all the RFs are essentially localised near the rotation center. This is the solution for $\alpha = 0.1$, $\beta = -0.9$.

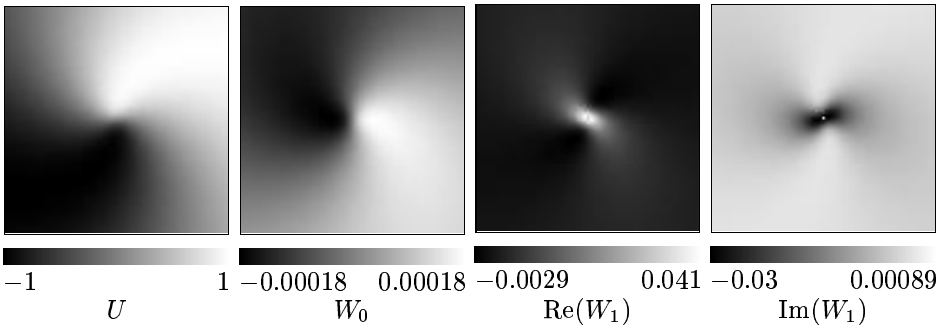

Figure 3: Solution for $\alpha = 0.1$, $\beta = 0.1$.

The character of the decrease the RFs at large ρ will be qualitatively different depending on the two negative roots of the characteristic equation (17). If they are both real, the decrease will be monotonic. If they are complex, the decrease will be oscillatory. On the (α, β) plane this cases are separated by the line $D \equiv (p/3)^3 + (q/2)^2 = 0$, also shown on Fig. 1. Fig. 4 illustrates what is happening in the region with oscillatory decrease. The behaviour of the RFs has changed qualitatively. Whereas the localisation of the RFs in Fig. 2 was almost entirely within the very tip of the spiral, RFs in Fig. 4 extend over the first winding. Another new feature is the 'halo', *i.e.* region around the innermost core, where the RFs have the opposite sign.

The next special line in (α, β)-plane is the line of the Eckhaus instability,

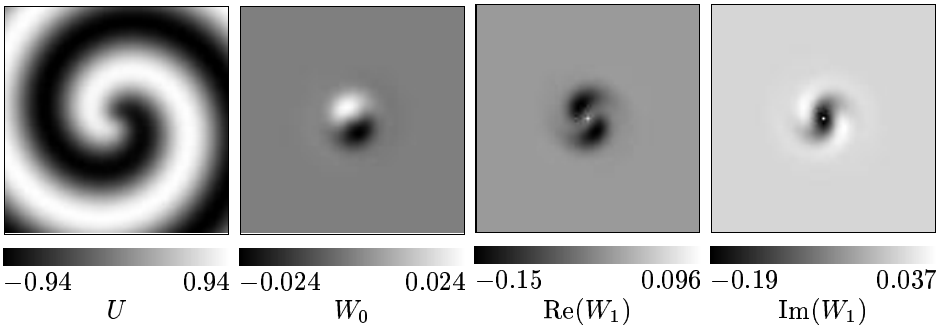

Figure 4: Solution for $\alpha = 0.5$, $\beta = 0.5$.

defined by equation $p = 0$. Beyond this line, the plane waves emitted by the spiral, are exponentially unstable with respect to longitudinal modulation. This implies that in this region, spiral wave solution should technically be unstable if considered on the whole plane. However, as it can be seen on Fig. 5, the localised RFs continue to exist even in that region, although their spatial extent grows further. Compare this observation with the sustained phenomenological stability of spiral waves beyond the Eckhaus limit, which was explained by the convective character of the Eckhaus instability [9].

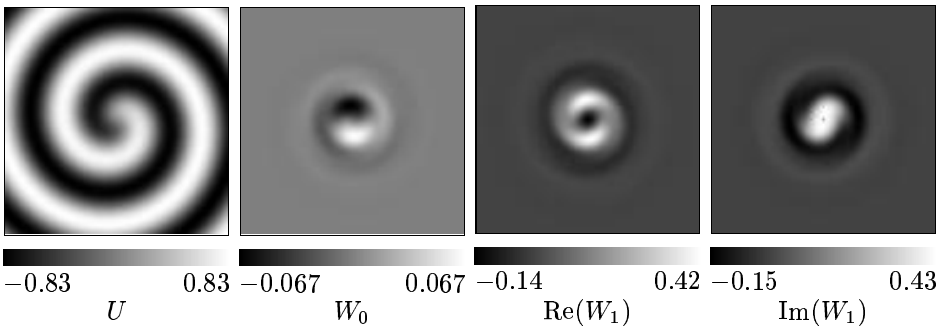

Figure 5: Solution for $\alpha = 1$, $\beta = 1$.

3 Conclusions

The obtained results suggest that the localisation of the response functions is a universal property of the spiral waves in the CGLE, at least in the region studied. This localisation only weakens near the line where the asymptotical wavelength grows, and beyond the Eckhaus limit, near the region of the absolute instability and turbulence. This evidence, by no means conclusive but encouraging, supports the viewpoint that the response functions remain localised as long as spiral wave solutions remain to exist and to be stable.

Changes in the behaviour of the spiral waves correlate with the change in the shape of the RFs. Approaching special regions in the (α, β) plane, such as the absolutely unstable region or the quasi-gradient line, is accompanied by characteristic changes in the shape of the RFs.

The RFs may be used to predict new qualitative features in the behaviour of the spiral waves. For example, the 'halo' around the central region of the RFs, in the Eckhaus unstable region, may mean a special behaviour of spiral waves with these parameters in the vicinity of a localised inhomogeneity, *e.g.* entrapment. This is a subject for further study.

Acknowledgements

We are grateful to Prof. A.V. Holden for the possibility to fulfill the computations for this work in his laboratory. Our participation in NEEDS-99 was supported in part by the Organising Committee of the conference and by Leeds University.

References

[1] A. M. Zhabotinsky and A. N. Zaikin. Spatial phenomena in an autooscillatory chemical system. In *Oscillatory Processes in Biological and Chemical Systems*, volume 2, pages 279–283, Pushchino, 1971. Nauka.

[2] R. A. Gray and J. Jalife. Spiral waves and the heart. *Int. J. of Bifurcation and Chaos*, 6(3):415–435, 1996.

[3] J. P. Keener. The dynamics of 3-dimensional scroll waves in excitable media. *Physica D*, 31(2):269–276, 1988.

[4] V. N. Biktashev, A. V. Holden, and H. Zhang. Tension of organizing filaments of scroll waves. *Phil. Trans. Roy. Soc. Lond. ser. A*, 347:611–630, 1994.

[5] V. N. Biktashev and A.V. Holden. Resonant drift of autowave vortices in 2D and the effects of boundaries and inhomogeneities. *Chaos Solitons & Fractals*, 5(3,4):575–622, 1995.

[6] I. V. Biktasheva, Y. E. Elkin, and V. N. Biktashev. Localised sensitivity of spiral waves in the Complex Ginzburg-Landau equation. *Phys. Rev. E*, 57(3):2656–2659, 1998.

[7] I. V. Biktasheva, Y. E. Elkin, and V. N. Biktashev. Resonant drift of spiral waves in the Complex Ginzburg-Landau equation. *J. Biol. Phys.*, 25(2):115–128, 1999.

[8] P. S. Hagan. Spiral waves in reaction-diffusion equations. *SIAM J. Appl. Math.*, 42(4):762–786, 1982.

[9] I. S. Aranson, L. Aranson, K. Kramer, and A. Weber. Stability limits of spirals and traveling waves in nonequilibrium media. *Phys. Rev. A*, 46(6):R2992–2993, 1992.